Monitoring the *Ex-Vivo* Expansion of Human Mesenchymal Stem/Stromal Cells in Xeno-Free Microcarrier-Based Reactor Systems by MIR Spectroscopy

Filipa Rosa and Kevin C. Sales
Engineering Faculty, Catholic University of Portugal, Rio de Mouro, Portugal

Joana G. Carmelo, Ana Fernandes-Platzgummer, and Cláudia L. da Silva
Dept. of Bioengineering and iBB-Institute for Bioengineering and Biosciences, Instituto Superior Técnico, Universidade De Lisboa, Av. Rovisco Pais, Lisboa 1049-001, Portugal

Marta B. Lopes
ISEL—Instituto Superior De Engenharia De Lisboa, Rua Conselheiro Emídio Navarro, 1, Lisboa 1959-007, Portugal

Institute of Telecommunications, Instituto Superior Técnico, Av. Rovisco Pais, Lisboa 1049-001, Portugal

Cecília R. C. Calado
ISEL—Instituto Superior De Engenharia De Lisboa, Rua Conselheiro Emídio Navarro, 1, Lisboa 1959-007, Portugal

DOI 10.1002/btpr.2215
Published online 00 Month 2015 in Wiley Online Library (wileyonlinelibrary.com)

Human mesenchymal stem/stromal cells (MSCs) have received considerable attention in the field of cell-based therapies due to their high differentiation potential and ability to modulate immune responses. However, since these cells can only be isolated in very low quantities, successful realization of these therapies requires MSCs ex-vivo *expansion to achieve relevant cell doses. The metabolic activity is one of the parameters often monitored during MSCs cultivation by using expensive multi-analytical methods, some of them time-consuming. The present work evaluates the use of mid-infrared (MIR) spectroscopy, through rapid and economic high-throughput analyses associated to multivariate data analysis, to monitor three different MSCs cultivation runs conducted in spinner flasks, under xeno-free culture conditions, which differ in the type of microcarriers used and the culture feeding strategy applied. After evaluating diverse spectral preprocessing techniques, the optimized partial least square (PLS) regression models based on the MIR spectra to estimate the glucose, lactate and ammonia concentrations yielded high coefficients of determination ($R^2 \geq 0.98$, ≥ 0.98, and ≥ 0.94, respectively) and low prediction errors (RMSECV $\leq 4.7\%$, $\leq 4.4\%$ and $\leq 5.7\%$, respectively). Besides PLS models valid for specific expansion protocols, a robust model simultaneously valid for the three processes was also built for predicting glucose, lactate and ammonia, yielding a R^2 of 0.95, 0.97 and 0.86, and a RMSECV of 0.33, 0.57, and 0.09 mM, respectively. Therefore, MIR spectroscopy combined with multivariate data analysis represents a promising tool for both optimization and control of MSCs expansion processes.* © 2015 American Institute of Chemical Engineers *Biotechnol. Prog.*, 000:000–000, 2015
Keywords: mesenchymal stem/stromal cells, MIR spectroscopy, high-throughput analysis

Introduction

Human mesenchymal stem/stromal cells (MSCs) have been widely studied for applications in regenerative medicine settings due to their ability to differentiate into diverse cell types, to produce trophic, paracrine and immunomodulatory factors, and to migrate towards sites of injured tissue, inflammatory and tumor sites.[1–3] MSCs have been isolated from tissues of perinatal origin (e.g., umbilical cord and placenta) and adult tissues like bone marrow (BM) and adipose tissue,[4] being able to differentiate into cell types of mesodermal origin (cartilage, bone, fat, among others).[5] Under specific conditions, MSCs also secrete bioactive molecules like cytokines, specific growth factors and antioxidants, which may act as immunomodulatory and promote tissue regeneration. To explore the intrinsic trophic activity of MSCs, the administration of these cells has been studied in numerous clinical trials, namely for knee cartilage injuries, Crohn's disease, acute respiratory distress syndrome, multiple sclerosis, limb and foot ischemia in diabetic patients, osteoarthrites, ulcerative colitis, and graft-vs.-host disease (http://clinicaltrials.gov accessed in Mars 2015).

Despite their great potential, MSCs are considerably rare in the human organism, representing, for instance, 0.001–0.01% of the mononuclear cells in BM. Considering that

Correspondence concerning this article should be addressed to C. R. C. Calado atccalado@deq.isel.pt.

Table 1. Advantages and Limitations of High-throughput MIR Spectroscopic Methods Compared with Traditional Methods

	MIR Spectroscopy	Traditional Methods
Reagents need	No	Yes (*e.g.,* eluents for chromatographic methods, enzymes and other reagents for enzymatic analysis)
Cost	Low	Medium to high
Sample processing before analysis	Simple (centrifugation and dehydratation)	Simple to complex
Speed of analysis	High (1 spectrum per min)	Low to medium
Automation	Yes	Yes or No (depending on the method)
Sample quantity	3–25 μL (depending of the microplate used)	Variable (depending on the method)
Type of analysis	Multiparametric	Uni or multiparametric
Methods for quantitative analysis	Multivariate data analysis	Univariate data analysis (usually)

average clinical doses are typically above 1 million MSCs per kg of patient body weight,[6] the expansion process of this type of cells represents an essential step for the translation of MSCs therapeutic potential.

To date, clinical-scale expansion of MSCs, which are anchorage dependent, has been performed in multilayer planar culture systems in the presence of fetal bovine serum (FBS) or human-sourced supplements, which present serious limitations of scalability and standardization, and are associated with safety risks and high labor costs.[7] Stirred bioreactors, combined with cell immobilization onto microcarriers, offer significant advantages over static systems, as they provide a homogeneous culture environment, monitoring and control procedures of key culture parameters and easy scalability.[8–10] Additionally, the use of well-defined xenogeneic (xeno)-free materials and formulations is essential for meeting rigorous quality and regulatory standards to robustly generate clinical-grade cells.[11] Overall MSC manufacturing depends on both biological and bioprocessing factors namely age and condition of the donor, cell source and isolation techniques used,[12,13] as well as on culture operation parameters (agitation, dissolved oxygen) and conditions (culture medium, surface coating, microcarrier type).[14,15] As small variations in the expansion process can cause serious changes in the MSCs final quality, a reproducible process and consequently an effective therapeutic product will only be ensured if appropriate monitoring and control of the MSCs expansion process is adopted.

Some of the variables that are commonly monitored in mammalian cell cultures include pH, temperature, dissolved oxygen concentration (DOC), and key analytes of cell metabolism like glucose, lactate, and ammonia.[16] Sensors for online monitoring of temperature, pH and DOC are well established. However, monitoring of the remaining critical variables of this bioprocess usually rely on multiple techniques, such as enzymatic assays, high-performance liquid chromatography and immuno-assays,[17] some of them based on time-consuming procedures. It is therefore critical to develop a new rapid and sensitive technique that enables the simultaneous acquisition of information concerning the critical variables of a given process (for control purposes) or multiple processes (for optimization purposes) and the whole molecular fingerprint of the complex culture matrices. In the spectroscopic field, vibrational spectroscopy such as Fourier transform infrared (FTIR) and Raman spectroscopies are able to detect the vibrational modes of biomolecules, thus holding the promise of playing an important role on the development of such ideal monitoring technique.

Vibrational spectroscopy detects the overall sample molecular fingerprint in a highly sensitive, rapid and economic way.[16–32] The technique does not require the use of any reagents or sample complex processing and a spectrum can be acquired in a time frame of a minute. Furthermore, the technique associated to multivariate analysis, e.g. partial least square (PLS) regression, allows the rapid quantification of several critical process variables from a single spectrum (i.e. the technique is multiparametric), in a highly sensitive way compared to conventional methods.[18–20] (Table 1).

The interest of monitoring animal cell cultures using vibrational spectroscopy is currently on its early stages. FTIR spectroscopy can be operated in the mid-infrared (MIR) and near-infrared (NIR) regions of the electromagnetic spectrum. Both MIR and NIR spectroscopies combined with PLS regression have been used to predict diverse metabolite concentrations in cultures of Chinese hamster ovary (CHO) cell lines, human embryonic kidney (HEK) cell lines, PC3 prostate cancer cells and Vero cell lines.[16,18–20,27–30] However, the errors of prediction obtained from these researchers are not fully comparable, as different cell lines, medium composition, bioreactor design, culture strategies, and spectral regions were used. To overcome this issue, Sandor et al.[18] compared the NIR and MIR spectral modes of acquisition combined with PLS regression to predict glucose on cultures of CHO cell lines, and found more than 50% error reduction with the MIR in relation to the NIR spectroscopy setup. This may result from the fact that the MIR region (between 4000 and 400 cm^{-1}) covers the fundamental vibrations of most common chemical bonds in biomolecules, where the known fingerprint region (bellow 1500 cm^{-1}) arises from the molecular skeleton (e.g., CC, COC, and COO), whereas the NIR region (between 14,000 and 4000 cm^{-1}) covers a more limited diversity of functional groups of biomolecules, detecting almost exclusively overtones and combination bands of the fundamental vibrations of groups containing the hydrogen atom (CH, NH, OH, and SH). Besides this advantage, MIR spectroscopy offers the possibility of high-throughput analysis, using microplates with multi-wells,[31,32] which could speed-up and promote optimization protocols of MSCs expansion processes, such as screening for optimal medium composition, initial cell densities, as well as evaluating the impact of scaling-up on cell features and final yield (Table 1).

Raman spectroscopy has also been successful applied for multi-analyte monitoring in mammalian cell cultures (e.g., Refs. 33–35). The main advantage over the above infrared techniques is the weaker absorption of water. However, in general, high concentrations of the target compounds are required to yield a detectable scattering, given the low probability of a molecule to undergo a Raman state transition. Moreover, at some wavelength ranges fluorescence of biological compounds present in the culture bulk may be generated which, being much more intense than Raman scattering,

dampens the measurements.[36] Indeed, PLS models to predict glucose, lactate and urea mixtures based on NIR spectra outperformed the equivalent regression models derived from Raman spectra.[37]

The present work evaluates the potential of high-throughput MIR spectroscopy to monitor the expansion process of human MSCs cultured in spinner flasks under xeno-free culture conditions with different microcarriers and using different feeding regimes. PLS regression models were developed to quantitatively predict the consumption of glucose and the production of lactate and ammonia along the expansion processes.

Materials and Methods

Samples

Human BM-derived MSCs were recovered from cryopreservation (as described in dos Santos et al.[38]) and cultured in culture flasks with StemPro® MSC SFM XenoFree medium (Life Technologies), supplemented with Penicillin (at a concentration of 0.025 U mL^{-1}) and Streptomycin (at a concentration of 0.025 μg mL^{-1}) (PenStrep, Life Technologies) and with GlutaMAX™-I CTS™ (Life Technologies) as a glutamine substitute. Cells were plated on T-flasks (Corning Falcon®) at an initial cell density between 3000 and 6000 and incubated at 37°C, 5%, in a humidified atmosphere. Culture medium was renewed every 3 or 4 days. When about 70 or 80% confluence was reached cells were detached with TrypLE™ Select (Life Technologies). Cells were then seeded and expanded during 13 days on plastic microcarriers under dynamic conditions, using Bellco® spinner flasks (Bellco Glass, Inc.) with a working volume of 80 mL, equipped with 90° paddles and a magnetic stirring bar. Three different MSCs expansion processes were implemented: Culture S, using plastic microcarriers (Pall SoloHill) previously coated with CELLstart™ CTS™ (Life Technologies) and Culture A1 and A2, using Synthemax® II microcarriers (Corning). These cultures were initiated with half the final volume (40 mL), which was then completed on the 3rd day, after which 25% of the medium was renewed every day for cultures S and A1 and every 2 days for culture A2.

Reference analysis

Samples were collected from cultures every day (with exception of day 2), being classified as before and after, if taken before or after the medium renewal, respectively.

Glucose, lactate and ammonia concentrations were determined using an automatic enzymatic analyzer YSI7100MBS (Yellow Springs Instruments).

Cell growth was monitored by harvesting the cells from the microcarriers with TrypLE solution in a Thermomixer comfort (Eppendorf) for 7 or 8 min at 37°C and 750 rpm. Then, IMDM with 10% fetal bovine serum (FBS) was added in a proportion of 1:3. Cells were separated from the microcarriers through filtration with a cell strainer (100 μm). Cell number and viability was determined by Trypan Blue exclusion method (Gibco).

Spectral acquisition

Supernatant samples of the cultures, preserved at −80°C, were thawed at room temperature and triplicates of 25 μL of each sample were transferred to a 96-wells Si plate for the FT-MIR high-throughput measurements. Samples were dehydrated before spectral acquisition in a desiccator under vacuum. The spectral data were collected using a FTIR Vertex 70 spectrometer (Burker, Germany) equipped with an HTS-XT accessory (Bruker, Germany). Forty scans in transmission mode, with a 4 cm^{-1} resolution, were collected in the wavenumber region between 500 and 4000 cm^{-1}. Each spectrum was baseline corrected with the OPUS software (Bruker, Germany) prior to data analysis.

Spectral data analysis

Data preprocessing, including multiplicative scatter correction (MSC), first and second order derivatives, was applied to spectral data prior to PLS modeling for predicting glucose, lactate and ammonia concentrations. Derivatives were computed using the Savitzky-Golay algorithm, with a filter window of 15 data points and a 2nd order polynomial fit. The performance of the PLS models was accessed through the evaluation of the root mean square error of cross-validation (RMSECV), root mean square error of prediction (RMSEP), the coefficient of determination (R^2) and the error as percentage of the concentration range (ER%), given by:

$$Error\ as\ \%\ of\ range = \frac{RMSEP}{range\ of\ concentration} \times 100$$

The best PLS model was selected regarding a high R^2, low calibration, validation and prediction errors and a low number of latent variables (LV) covering enough data variance. All calculations were performed using Matlab R2012b (Matworks, Natick, MA).

Results and Discussion

The expansion of MSCs requires not only the optimization of the culture general conditions but also the development of new monitoring methods that can offer sensitive, robust, rapid and economic monitoring of the expansion process for control purposes. One example of the critical relevance of controlling the MSCs expansion process is the high sensitivity of MSCs to their environment. It has been reported that a glycolytic metabolism, obtained e.g. at low oxygen tensions and leading to accumulation of lactate, is associated to proliferation of stem and progenitors cells, including human MSCs, whereas the predominance of an oxidative phosphorylation under higher oxygen tensions is associated to stem cell differentiation.[39] Monitoring cell metabolism in MSCs cultures is thus of major importance towards the maximization of cell yield, while maintaining the intrinsic cell therapeutic features.

The effect of different parameters that are critical for microcarrier-based stirred cultures was evaluated in three different expansion cultures, using different microcarriers and feeding regimes: Culture S, using SoloHill plastic microcarriers which are manually precoated with a xeno-free attachment substrate prior to cell culture and Culture A1 and A2, using ready-to-use Synthemax®II microcarriers (peptide-conjugated plastic microcarriers); in culture S and A1, 25% of the medium was renewed every day after the 3rd day, whereas in Culture A2, 25% of the medium was renewed every 2 days (Figure 1). Microcarrier properties can influence the expansion process and thus, they must allow

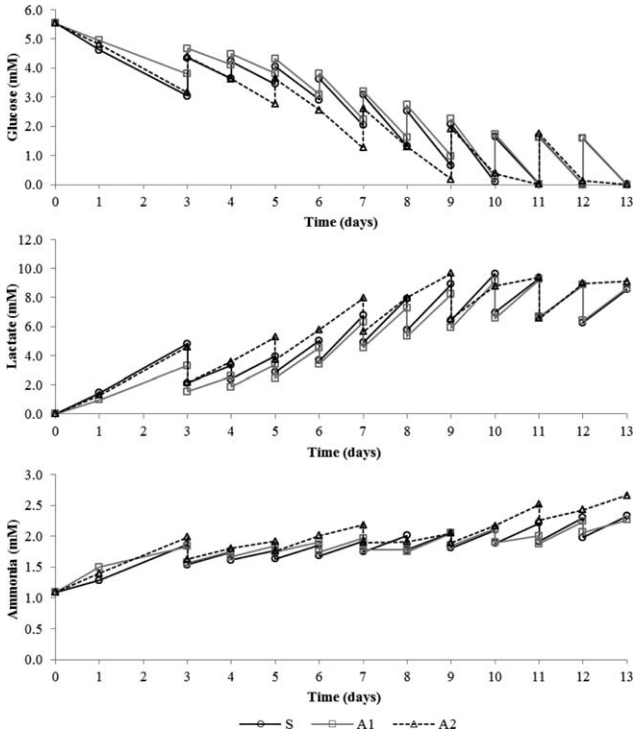

Figure 1. Glucose, lactate and ammonia concentration throughout BM-MSC expansion in spinner flask cultures using precoated SoloHill microcarriers (culture S), Synthemax®II microcarriers (culture A1 and A2), with medium renewal everyday (culture S and A1) or every 2 days (culture A2) after the 3rd day.

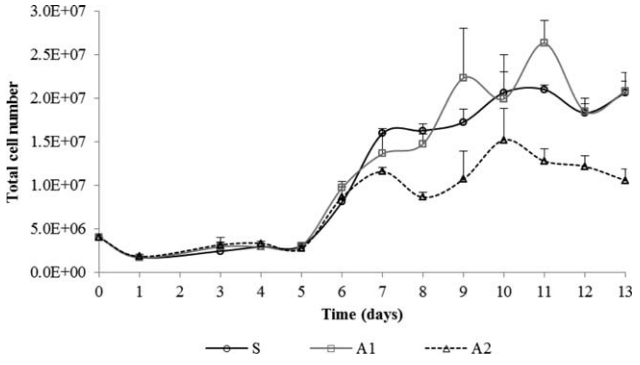

Figure 2. Concentration of BM-MSC in xeno-free spinner flask cultures with pre-coated SoloHill microcarriers (culture S) and Synthemax II microcarriers (culture A1 and A2). Culture medium was renewed every day (culture S and A1) or every 2 days (culture A2) after 3rd day of culture. Standard deviation (SD) values are represented along with the mean values of two replicate countins for each time point (1 donor).

efficient MSCs adhesion and subsequent expansion. In general, Cultures S and A1, in which different microcarriers were used and the medium was renewed every day, exhibited similar glucose and metabolites profiles, with slightly higher lactate production and glucose consumption in culture S in the first days (Figure 1). However, this difference was not associated to relevant distinction in cell growth between both cultures (Figure 2). Culture A2 presented lower concentrations of glucose and higher concentrations of lactate and ammonia in relation to the other two cultures, as expected by the less frequent feeding regime (Figure 1). All cultures were characterized by higher specific glucose consumption and lactate production in the first days of culture, reaching maximum values in the fourth or fifth day that decreased from then on (data not shown); a metabolic profile that has been previously verified in other works of microcarrier-based MSCs cultures.[40] These values correspond to apparent yields of lactate from glucose around 2.0 ± 0.2 in the first 5 days of culture and 1.6 ± 0.2 in the following days, suggesting a shift to a metabolism where glucose was more efficiently consumed for energy production.

Table 2. PLS Regression Models Based on Spectral Data Preprocessed with Different Techniques, for the Glucose Prediction During MSC Cultures Conducted on Pre-coated SoloHill Microcarriers with the Media Renewed Every Day (Culture S) (MSC—Multiplicative Scatter Correction)

	Without Preprocessing		MSC		1st derivative		2nd derivative	
LV	R^2	RMSECV	R^2	RMSECV	R^2	RMSECV	R^2	RMSECV
2	0.79	0.70	0.81	0.66	0.95	0.34	0.95	0.34
3	0.92	0.43	0.94	0.37	0.97	0.26	0.96	0.31
4	0.94	0.36	0.95	0.32	0.98	0.22	0.98	0.23
5	0.96	0.32	0.96	0.32	0.99	0.18	0.98	0.19
6	0.96	0.29	0.97	0.25	0.99	0.18	0.99	0.18
7	0.97	0.28	0.98	0.23	0.99	0.17	0.99	0.15

The three independent cultures presented similar growth profiles until the sixth day of culture, presenting a lag phase until the fifth day (Figure 2). From then on, Cultures S and A1, with daily medium renewal, showed identical growth profiles, reaching higher cell densities than culture A2, around 2×10^5 cells mL^{-1}. The lower productivity in Culture A2 until the 8th day may be due to the limitation of growth factor(s) or nutrient starvation, other than glucose, as according to the glucose concentration profile, about 3 mM of glucose was still present when growth started to be compromised. On the other hand, lactate and ammonia at this time point were at non-inhibitory levels (Figures 1B,C). Overall, in all cultures, regardless the feeding regimen, glucose starvation occurs from day 9 to 10 onwards suggesting that during that period the levels of this nutrient were limited for cell growth/maintenance. According to the lactate and ammonia concentration profiles, slightly higher concentrations of these by-products were reached in Culture A2. Growth inhibitory concentrations have been reported to be 35.4 mM for lactate and 2.4 mM for ammonia.[41] Although lactate did not reach such inhibitory level, cells seem to have increased ammonia production after glucose depletion, reaching inhibitory values (2.7 mM) at the end of culture. Furthermore, after the 9th day, all cultures started to form cell-carrier aggregates due to a great level of confluence on the beads surface, which became larger with time, particularly in cultures S and A1 that achieved higher cell densities (data not shown). Importantly, after spinner flask cultures, we verified that expanded MSCs retained their immunophenotype and multilineage differentiation capacity (data not shown), as previously reported by our group.[40,42]

PLS regression models were developed to estimate glucose, lactate and ammonia concentrations from the MIR spectra for each of the three cultures (Table 2). PLS enables predicting a set of dependent variables (e.g. the concentration of glucose) from a very large set of independent variables or predictors (e.g., MIR wavenumbers), by extracting a set of orthogonal factors from the predictors designated by latent variables (LV) which have the best

Table 3. PLS Regression Models for Glucose, Lactate, and Ammonia Concentration Prediction, Using the First Derivative as Spectral Preprocessing, for MSC Cultured on Precoated SoloHill Microcarriers (Culture S) or on Synthemax® II Microcarriers (Culture A1 and A2), with Daily Media Renewal (Culture S and A1) or Every 2 Days (Culture A2)

Culture	Analyte	LV	R^2	RMSECV	Concentration range (mM)	Error as % of the concentration range
S	Glucose	4	0.98	0.22	0.01–4.61	4.7
	Lactate	4	0.98	0.36	1.39–9.65	4.4
	Ammonia	5	0.95	0.06	1.29–2.33	5.7
A1	Glucose	4	0.98	0.23	0.00–5.54	4.2
	Lactate	5	0.98	0.39	0.02–9.24	4.3
	Ammonia	5	0.94	0.06	1.09–2.27	5.4
A2	Glucose	3	0.99	0.17	0.01–5.54	3.2
	Lactate	3	0.99	0.25	0.02–9.68	2.5
	Ammonia	4	0.94	0.09	1.09–2.67	5.7

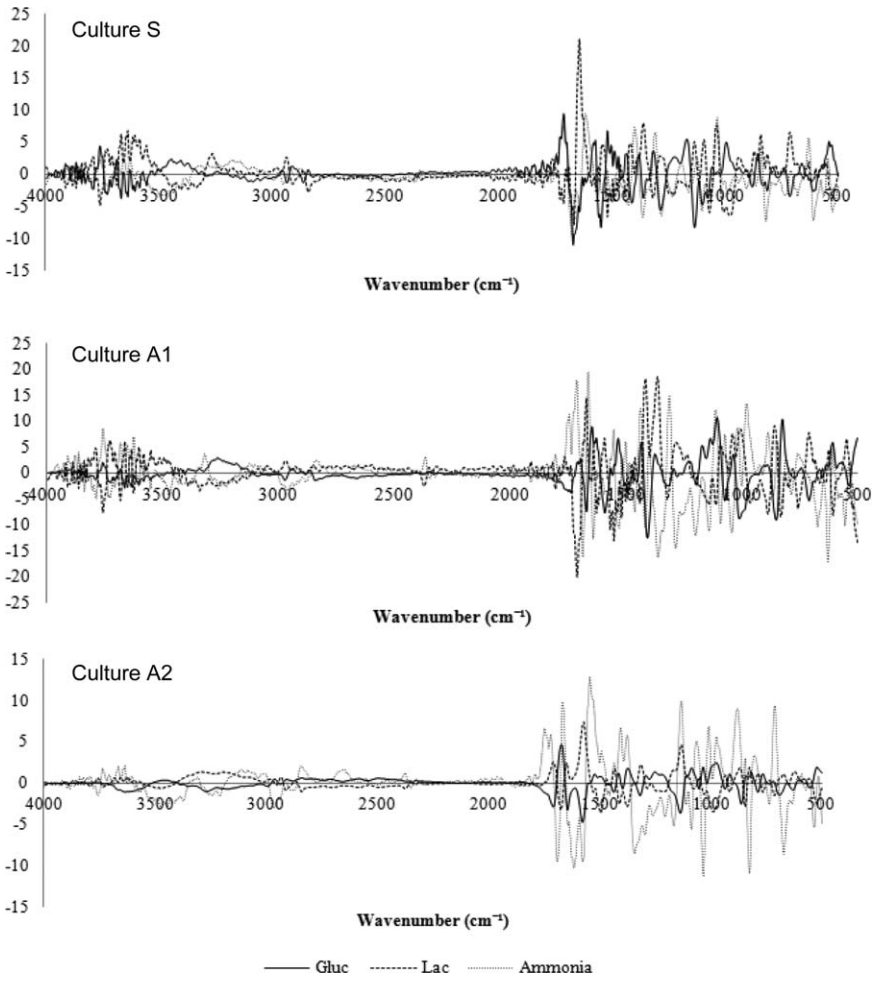

Figure 3. Regression vector from the best PLS model built for glucose, lactate and ammonia on cultures of BM-MSC conducted on pre-coated SoloHill microcarriers (culture S) or on Synthemax® II microcarriers (culture A1 and A2), with daily media renewal (culture S and A1) or every 2 days (culture A2).

predictive power.[43] As each culture presented a low number of samples (up to 68 for each culture, including the three replicates for each sample), a leave-one-out (LOO) cross-validation strategy was applied. To enhance the predictive ability of the PLS models, the spectral preprocessing techniques MSC and spectral derivatives were evaluated. MSC can theoretically minimize physical effects, such as light scattering resulting from particles of different sizes,[44] which could appear during the cell pellet dehydration process conducted before spectral acquisition. Derivatives can enhance the information in data, due to increased resolution of bands overlapping, while minimizing physical interferences. However, two major drawbacks of applying derivatives are the reduction of the signal scale and noise amplification. To minimize noise amplification the spectrum was smoothed with a Savitzky–Golay filter. Table 2 summarizes the performance of PLS models built to estimate the glucose concentration on culture S, after preprocessing with MSC and first and second derivatives. The application of MSC resulted in models with improved performance in relation to models build without that preprocessing technique. The application of first derivative also improved the models performance, while the application of the second derivative did not significantly improve the models' predictive ability compared to the application of the first derivative. The same has been observed for the lactate and ammonia PLS models, so that the first derivative was selected as the preprocessing method of choice.

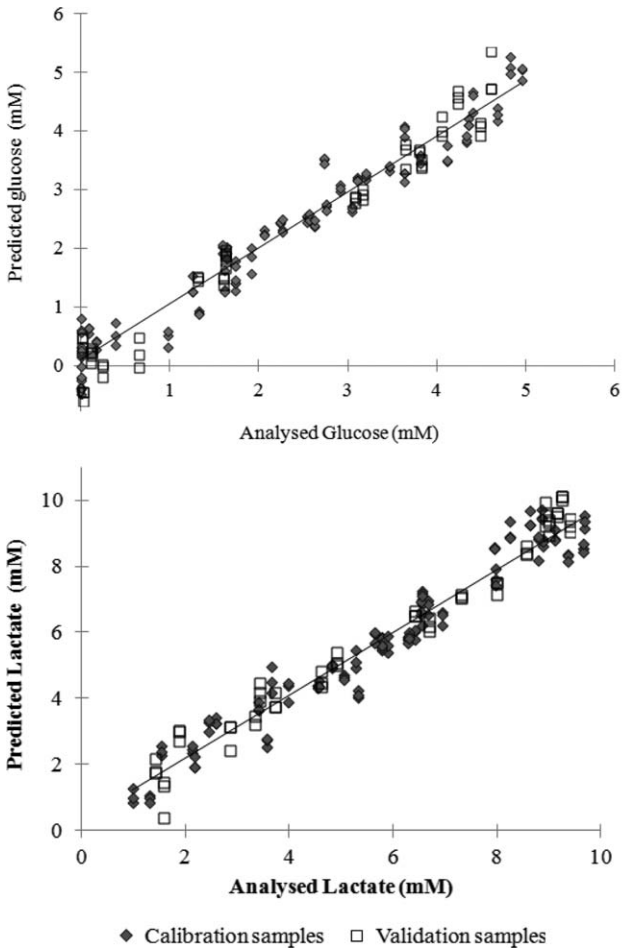

Figure 4. Glucose and lactate concentrations predicted by global PLS regression models, based on MIR spectra obtained from three independent MSC expansion processes, in relation to the reference values obtained by conventional methods.

Besides a high R^2 and a low error (e.g., RMSECV), a PLS model should also be based on low number of LV, covering enough data variance.[36,45] A low number of LVs can result in underfitting especially if the variance represented in data is low, while a high number can lead to overfitting, which means reduced model predictive ability outside the conditions used for calibration. A high-accuracy PLS model was built to predict the glucose concentration during culture S, using 4 LVs explaining 98% of data variance, and yielding a R^2 of 0.98 and a RMSECV of 0.22 mM. This error is lower than those obtained by other authors developing of PLS models for estimating the glucose concentration in mammalian cultures based on MIR spectra obtained either from an ATR MIR probe or a 96-wells Si plate, producing errors between 0.5 and 2.17 mM.[16,18,19] High-accuracy PLS models to predict lactate and ammonia concentrations were also obtained for culture S, considering 4 and 5 LVs explaining 98 and 95% of data variance, yielding a R^2 of 0.98 and 0.95 and RMSECV of 0.36 and 0.06 mM, respectively (Table 2). Previous works on the development of PLS models based on MIR spectra to predict the lactate concentrations based on MIR spectra, produced higher errors of prediction, i.e., $\geq$0.6 mM.[16,18,19,46]

PLS models built for the three analytes for culture A1 yielded very similar results as the models built for culture S, whereas PLS models built for culture A2 presented slightly better performances to predict glucose and lactate concentration and slightly worse to predict the ammonia concentration, regarding the R^2 and RMSECV (Table 3). The similarities between the PLS models' performance (concerning R^2 and RMSECV) for cultures S and A1 are according to growth similarities between these cultures, whereas culture A2 showing a different growth profile yielded a different PLS models performance. The similarities between PLS models for culture S and A1 and the differences between these cultures and culture A2 are also reflected in the regression vectors of the corresponding PLS models (Figure 3). For example, the region between 2800 and 3800 cm^{-1} shows a contribution to the PLS models for glucose, lactate and ammonia of cultures S and A1, as opposed to culture A2. This region reflects mostly stretching vibrations between X-H groups (where X is C, O or N), present e.g., in hydroxyl groups on glucose, lactate, and NH on ammonia. Therefore, the present PLS model performances may be dependent of the expansion process characteristics.

All PLS models from the three cultures had a strong contribution from the spectral region between 500 and 1900 cm^{-1}. The region between 1800 and 1500 cm^{-1} reflects mainly stretching vibrations of double bonds between C═X, where X is C, O or N), e.g. C═O present in the aldehyde group of glucose and in the carboxylic group of lactic acid. The region between 1500 and 500 cm^{-1} reflects a variety of overlapped vibrations, being designated as the fingerprinting region.[47] The strong contribution of this region for the PLS models developed for glucose, lactate and ammonia most probably reflects the effect of the stem cells metabolism on the culture medium matrix.

One factor that must be taken into account when evaluating PLS models for different parameters while studying a cell culture, is that some of these parameters are highly correlated with each other (for instance lactate is a product of glucose fermentation). The different feeding conditions and microcarriers applied to the culture runs can be very useful to break the correlations between the compounds under study.[18,28] Also some useful information can be obtained through the PLS regression vector, as it provides information about the spectral regions that contribute the most for model building. The regression vectors obtained for glucose and lactate are more similar compared to the regression vector obtained from the ammonia model (Figure 3), as glucose and lactate have similar molecular compositions, thus absorbing in similar wavelength regions. Nevertheless, the PLS models for the three analytes provided distinct regression vectors.

An additional global PLS model was developed using all samples from the three independent cultures (176 samples including replicates), performed under different conditions, either regarding the type of microcarriers used or the frequency of the medium renewal. This PLS model therefore accounted for a high variability in terms of culture conditions. Because of the larger number of samples available for the glucose and lactate model, the calibration and test sets consisted of samples randomly chosen from the three cultures, where the calibration set included about 2/3 of the available samples and the test set about 1/3 of the samples. The ammonia model was built using a LOO cross-validation strategy as before. When comparing the PLS models using all available samples with the models developed using a single culture, a general decrease in the predictive ability was

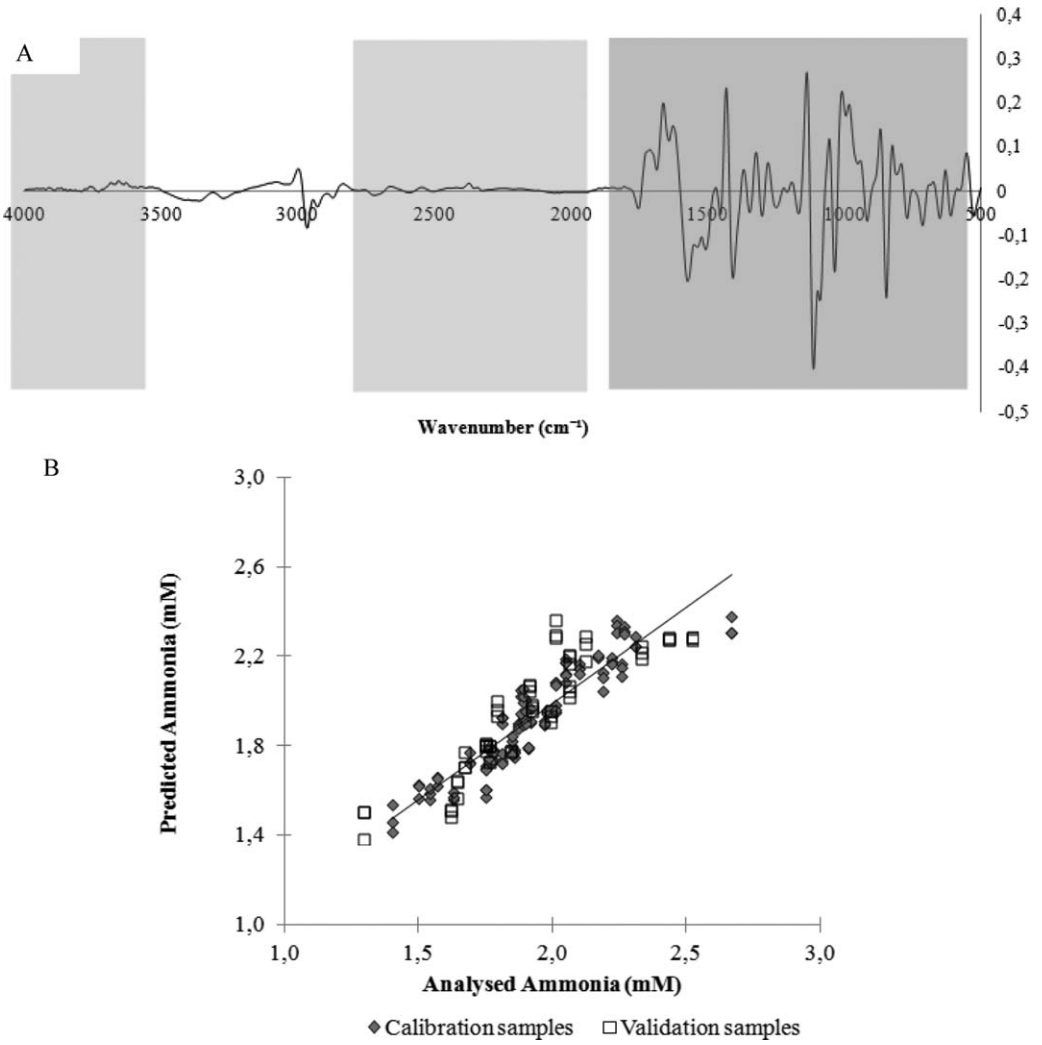

Figure 5. Ammonia global PLS model based on spectral data from the three cultures. (A) Regression vector from the PLS model considering the entire spectral region; B) Ammonia concentration predicted by global PLS regression model considering the spectral region without the regions between 3500 and 4000 cm^{-1} and between 1950 and 2700 cm^{-1}, in relation to the reference values obtained by conventional methods.

observed, as expected (Figure 4, Table 3). Nevertheless, still accurate global PLS models were obtained. A glucose model based on 5 LVs was obtained (Figure 4), yielding a RMSEP of 0.33 mM and a R^2 of 0.95. For the lactate prediction (Figure 4), a model based on 5 LVs resulted in a RMSEP of 0.57 mM and a R^2 of 0.97. These errors obtained by modeling MIR spectra from three different cultures are in agreement with previous errors obtained by other authors.[16,18,19]

The global PLS model obtained for ammonia yielded considerably worse predictions when compared to the PLS models obtained for each individual culture. A model with 5 LVs resulted in a RMSECV of 0.70 mM and a R^2 of 0.78. As an attempt to improve the model predictive performance, two models with selected spectral regions were built: first, using only the spectral region between 500 and 1900 cm^{-1}, as the regression vector highlights this region as the one with the highest contribution for model development (Figure 5A); second, by eliminating the spectral regions between 3500 and 4000 cm^{-1} and between 1950 and 2700 cm^{-1}, which presented a lower contribution for the model development (Figure 5A). The model using only the spectral region between 500 and 1900 cm^{-1} showed no improvements, which may indicate that even showing a lower contribution to the model, the excluded spectral regions still provide meaningful information. For the second model, for which two spectral regions were eliminated, the predictive ability significantly improved. For this last model based on 5 LVs a RMSECV of 0.09 mM and a R^2 of 0.86 were obtained (Figure 5B).

In resume, FT-MIR spectroscopy, combined with multivariate data analysis, proved to be an ideal tool to monitoring MSCs expansion in bioreactors, as it enables a rapid estimation of several critical parameters at once, in an economic and high-throughput way. The knowledge on the process can therefore be substantially increased in a near real-time fashion.

Acknowledgments

The Innovation Agency (Portugal) is acknowledged through the financial support of the CLARO project. Marta B. Lopes gratefully acknowledges the post-doctoral scholarship from FCT (SFRH/BPD/73758/2010). The present work was partly conducted in the Health and Engineering Laboratory resulted from the Protocol between *Universidade Católica Portuguesa* and the *Instituto Politécnico de Lisboa*.

Literature Cited

1. Murphy MB, Moncivais K, Caplan AI. Mesenchymal stem cells: environmentally responsive therapeutics for regenerative medicine. *Exp Mol Med.* 2013;45:e54.
2. Jacobs SA, Roobrouck VD, Verfaillie CM, Van Gool SW. Immunological characteristics of human mesenchymal stem cells and multipotent adult progenitor cells. *Immunol Cell Biol.* 2013; 91:32–39.
3. De Miguel MP, Fuentes-Julián S, Blázquez-Martínez A, Pascual CY, Aller MA, Arias J, Arnalich-Montiel F. Immunosuppressive properties of mesenchymal stem cells: advances and applications. *Curr Mol Med.* 2012;12:574–591.
4. Strioga M, Viswanathan S, Darinskas A, Slaby O, Michalek J. Same or not the same? Comparison of adipose tissue-derived versus bone marrow-derived mesenchymal stem and stromal cells. *Stem Cells Dev.* 2012; 21:2724–2752.
5. Pittenger MF, Mackay AM, Beck SC, Jaiswal RK, Douglas R, Mosca JD, Moorman MA, Simonetti DW, Craig S, Marshak DR. Multilineage potential of adult human mesenchymal stem cells. *Science.* 1999;284:143–147.
6. Parekkadan B, Milwid JM. Mesenchymal stem cells as therapeutics. *Annu Rev Biomed Eng.* 2010;12:87–117.
7. Bieback K, Schallmoser K, Klüter H, Strunk D. Clinical protocols for the isolation and expansion of mesenchymal stromal cells. *Transfus Med Hemother.* 2008;35:286–294.
8. dos Santos F, Andrade PZ, Silva CL, Cabral JM. Scaling-up ex vivo expansion of mesenchymal stem/stromal cells for cellular therapies. In: Chase LG, Vemuri MC, editors. Mesenchymal Stem Cell Therapy. Humana Press, New York; 2013;1–14.
9. Rodrigues CA, Fernandes TG, Diogo MM, da silva CL, Cabral JM. Stem cell cultivation in bioreactors. *Biotechnol Adv.* 2011; 29:815–829.
10. Kirouac DC, Zandstra PW. The systematic production of cells for cell therapies. *Cell Stem Cell.* 2008;3:369–381.
11. Kinzebach S, Bieback K. Expansion of mesenchymal stem/stromal cells under xenogenic-free culture conditions. *Adv Biochem Eng Biotechnol.* 2013;129:33–57.
12. Busser H, De Bruyn C, Urbain F, Najar M, Pieters K, Raicevic G, Meuleman N, Bron D, Lagneaux L. Isolation of adipose derived stromal cells without enzymatic treatment: expansion, phenotypical and functional characterization. *Stem Cells Dev.* 2014;23:2390–2400.
13. Le Blanc K, Rindgén O. Immunobiology of human mesenchymal stem cells and future use in hematopoietic stem cell transplantation. *Biol Blood Marrow Transplant.* 2005;1:321–334.
14. Chen AK, Reuveny S, Oh SK. Application of human mesenchymal and pluripotent stem cell microcarrier cultures in cellular therapy: achievements and future direction. *Biotechnol Adv.* 2013;31:1032–1046.
15. Hoch AI, Leach JK. Concise review: optimizing expansion of bone marrow mesenchymal stem/stromal cells for clinical applications. *Stem Cells Transl Med.* 2014;3:643–652. doi:10.5966/sctm.2013-0196.
16. Rhiel M, Ducommum P, Bolzonella I, Marison I, Stockar U. Real-time in situ monitoring of freely suspended and immobilized cell cultures based on mid-infrared spectroscopic measurements. *Biotechnol Bioeng.* 2002;77:174–185.
17. Harthun S, Matischak K, Friedl P. Simultaneous prediction of human antithrombin III and main metabolites in animal cell culture processes by near-infrared spectroscopy. *Biotechnol Techn.* 1998;23:393–398.
18. Sandor M, Rüdinger F, Bienert R, Grimm C, Solle D, Scheper T. Comparative non-invasive monitoring via infrared spectroscopy for mammalian cell cultivations. *J Biotechnol.* 2013;68: 636–645.
19. Sellick CA, Hansen R, Jarvis RM, Maqsood AR, Stephens GM, Dickson AJ, Goodacre R. Rapid monitoring of recombinant antibody production by mammalian cell cultures using Fourier transform infrared spectroscopy and chemometrics. *Biotechnol Bioeng.* 2010;106:432–442.
20. Rhiel MH, Amrhein MI, Marison IW, von Stockar U. The influence of correlated calibration samples on the prediction performance of multivariate models based on mid-infrared spectra of animal cell cultures. *Anal Chem.* 2002;74:5227–5236.
21. Hakemeyera C, Straussa U, Werza S, Joseb GE, Folque F, Menezes JC. At-line NIR spectroscopy as effective PAT monitoring technique in Mab cultivations during process development and manufacturing. *Talanta.* 2012;90:12–21.
22. Chen Z, Lovett D, Morris J. Process analytical technologies and real time process control a review of some spectroscopic issues and challenges. *J Process Control.* 2011;21:1467–1482.
23. Roggo Y, Chalus P, Maurer L, Lema-Martinez C, Edmond A, Jent N. A review of near infrared spectroscopy and chemometrics in pharmaceutical technologies. *J Pharma Biomed Anal.* 2007;44:683–700.
24. Cervera AE, Petersen N, Lantz AE, Larsen A, Gernaey KV. Application of near-infrared spectroscopy for monitoring and control of cell culture and fermentation. *Biotechnol Prog.* 2009; 25:1561–1581.
25. Landgrebe D, Haake C, Höpfner T, Beutel S, Hitzmann B, Beutel S, Hitzmann B, Scheper TM, Reardon KF. On-line infrared spectroscopy for bioprocess monitoring. *Appl Microbiol Biotechnol.* 2010;88:11–22.
26. Roychoudhury P, Harvey LM, McNeil B. The potential of mid infrared spectroscopy (MIRS) for real time bioprocess monitoring. *Anal Chim Acta.* 2006;571:159–166.
27. Clavaud M, Roggo Y, Von Daeniken R, Liebler A, Schwabe JO. Chemometrics and in-line near infrared spectroscopic monitoring of a biopharmaceutical Chinese hamster ovary cell culture: prediction of multiple cultivation variables. *Talanta.* 2013; 111:28–38.
28. Petiot E, Bernard-Moulin P, Magadoux T, Gény C, Pinton H, Marc A. In-situ quantification of microcarrier animal cultures using near-infrared spectroscopy. *Process Biochem.* 2010;45: 1832–1836.
29. Card C, Hunsaker B, Smith T, Hirsch J. Near-infrared spectroscopy for rapid, simultaneous monitoring. *BioProcess Int.* 2008; 6:59–67.
30. Harthun S, Matischak K, Friedl P. Determination of recombinant protein in animal cell culture supernatant by near-infrared spectroscopy. *Anal Biochem.* 1997;251:73–78.
31. Sales KC, Rosa F, Sampaio PN, Fonseca LP, Lopes MB, Calado CRC. In situ near-infrared (NIR) versus high-throughput mid-infrared (MIR) spectroscopy to monitor biopharmaceuticals production. *J Appl Spectrosc* 2015;69:760–72.
32. Scholz T, Lopes VV, Calado CRC. High-throughput analysis of the plasmid bioproduction process in *Escherichia coli* by FTIR spectroscopy. *Biotechnol Bioeng.* 2012;109:2279–2285.
33. Abu-Absi NR, Kenty BM, Cuellar ME, Borys MC, Sakhamuri S, Strachan DJ, Hausladen MC, Li ZJ. Real time monitoring of multiple parameters in mammalian cell culture bioreactors using an in-line Raman spectroscopy probe. *Biotechnol Bioeng.* 2011; 108:1215–1221.
34. Moretto J, Smelko JP, Cuellar M, Berry B, Doane A, Ryll T, Wiltberger K. Process Raman spectroscopy for in-line CHO cell culture monitoring. *Am Pharm Rev.* 2011;5:18–25.
35. Whelan J, Craven S, Gennon B. In situ spectroscopy for simultaneous monitoring of multiple process parameters in mammalian cell culture bioreactors. *Biotechnol Prog.* 2012;28:1355–1362.
36. Teixeira AP, Oliveira R, Alves PM, Carrondo MJT. Advances in on-line monitoring and control of mammalian cell cultures: supporting the PAT initiative. *Biotechnol Adv.* 2009; 27:726–732.
37. Ren M, Arnold MA. Comparison of multivariate calibration models for glucose, urea, and lactate from near-infrared and Raman spectra. *Anal Bioanal Chem.* 2007;387:879–888.
38. dos Santos F, Andrade PZ, Boura JS, Abecasis MMA, da Silva CL, Cabral JMS. Ex vivo expansion of human mesenchymal stem cells: a more effective cell proliferation kinetics and metabolism under hypoxia. *J Cell Physiol.* 2010;223:27–35.
39. Sart S, Agathos SN, Li Y. Process engineering of stem cell metabolism for large scale expansion and differentiation in bioreactors. *Biochem Eng J.* 2014;84:74–82.
40. dos Santos FD, Andrade PZ, Abecasis MM, Gimble JM, Chase LG, Campbell AM, Boucher S, Vemuri MC, Silva CL, Cabral JM. Toward a clinical-grade expansion of mesenchymal stem cells from human sources: a microcarrier-based culture system

under xeno-free conditions. *Tissue Eng C Methods*. 2011;17: 1201–1210.
41. Schop D, Janssen FW, van Rijn LD, Fernandes H, Bloem RM, de Bruijn JD, van Dijkhuizen-Radersma R. Growth, metabolism, and growth inhibitors of mesenchymal stem cells. *Tissue Eng A*. 2009;15:1877–1886.
42. Carmelo JG, Fernandes-Platzgummer A, Diogo MM, da Silva CL, Cabral JMS. A xeno-free microcarrier-based stirred culture system for the scalable expansion of human mesenchymal stem/stromal cells isolated from bone marrow and adipose tissue. *Biotechnol J*. 2015;10:1235–1247. doi: 10.1002/biot. 201400586
43. Abdi H. Partial least squares regression and projection on latent structure regression (PLS Regression). *Wiley Interdiscip Rev Comput Stat*. 2010;2:387–515.
44. Helland S, Naes T, Isaksson T. Related version of multiplicative scatter correction method for preprocessing spectroscopic data. *Chemometr Intell Lab Syst*. 1995;9:233–241.
45. Haaland DM, Thomas EV. Partial least-squares methods for spectral analysis. 1. Relation to other quantitative calibration methods and the extraction of qualitative information. *Anal Chem*. 1988;60:1193–1202.
46. Capito F, Zimmer A, Skudas R. Mid-infrared spectroscopy-based analysis of mammalian cell culture parameters. *Biotechnol Prog*. 2015;31:578–586.
47. Bellisola G, Sorio C. Infrared spectroscopy and microscopy in cancer research and diagnosis. *Am J Cancer Res*. 2012;2:1–21.

Manuscript received Mar. 18, 2015, and revision received Dec. 1, 2015.